Materials and Structures (2021) 54:44
https://doi.org/10.1617/s11527-021-01633-w

ORIGINAL ARTICLE

Thermal and hydrothermal treatment of UHPC: influence of the process parameters on the phase composition of ultra-high performance concrete

Julia von Werder · Sebastian Simon · André Gardei · Patrick Fontana · Birgit Meng

Received: 2 July 2020 / Accepted: 17 January 2021 / Published online: 10 February 2021

Abstract Several studies show that thermal and hydrothermal treatment can further improve the excellent properties of UHPC in terms of mechanical strength and durability. While for the thermal treatment the increase in strength is attributed to an intensified pozzolanic and hydraulic reaction, for the hydrothermal treatment previous studies accredited it mostly to the formation of tobermorite. In the presented study thermal and hydrothermal treatment of UHPC samples was systematically varied and the phase formation analysed related to the strength development of a reference sample cured for 28 days in water. For the thermal treatment the results show that the strength increase depends on the protection against desiccation and can be ascribed to an improved pozzolanic reaction of the siliceous fillers. To achieve a significant enhancement of strength, a pre-storage time of few days and a long dwell time at elevated temperature/pressure are required. For the hydrothermal treatment already heating the specimens up to 185 °C in saturated steam followed by an immediate cooling leads to a substantial increase in compressive strength. Pre-storage time did not affect the result as far as a minimum of several hours is guaranteed. The improved performance is due to an increase in the pozzolanic and hydraulic reaction. Surprisingly, tobermorite was only found within a very thin layer at the surface of the sample, but not in the bulk. Sulphate and aluminium stemming from the decomposition of the ettringite are bound in the newly formed phases hydroxylellestadite and hydrogarnet.

Keywords UHPC · Thermal treatment · Hydrothermal treatment · Compressive strength · Phase development · Durability · Tobermorite · Hydroxylellestadite · Hydrogarnet

1 Introduction

1.1 UHPC

Ultra-high-performance concrete (UHPC) is characterised by a compressive strength systematically greater than 120 MPa [1, 2], in extreme cases even possibly attaining 400 MPa [3]. The high strength is attributed to a high binder content, an optimized graduation of granular constituents and the use of highly effective additions such as microsilica. Furthermore, UHPC is distinguished by a very low water/cement (w/c) ratio usually less than 0.3. The required workability and even self-compacting properties are

J. von Werder (✉) · S. Simon · A. Gardei · B. Meng
Bundesanstalt für Materialforschung und -prüfung (BAM), Berlin, Germany
e-mail: julia.von-werder@bam.de

P. Fontana
RISE Research Institutes of Sweden, Stockholm, Sweden

adjusted by highly efficient superplasticizers like PCE (polycarboxylate ether). Low w/c ratio and good workability result in a very dense structure, which in turn is also related to low permeability and an exceptional durability compared to ordinary concrete.

Extensive research in the last decades lead to the application of UHPC in various fields like for example in bridges, façade elements or pier repair [4–6]. In most of the applications the building components were produced in precast concrete element plants and assembled on site [7].

Due to the high input of cement and pozzolanic fillers the production of UHPC is cost-intensive. The slender and lightweight constructions realized with UHPC allow however material savings, which can overcompensate the higher material costs. In addition, the lower life cycle costs resulting from the high durability of UHPC can improve its sustainability compared to ordinary concrete [8]. Many studies further showed that more environmentally friendly and cost efficient UHPC can be produced by using locally available supplementary cementitious materials (SCMs) [9] or replacing cement by inert fillers [10]. The slower strength development of UHPC containing high amounts of pozzolanic or latent-hydraulic SCMs can be compensated by a thermal treatment [11].

1.2 Thermal treatment

Thermal treatment of UHPC, often referred to as 'heat curing' or 'steam curing', is recommended in specific cases for a more robust and time efficient production of prefabricated elements [12–14]. Since 'curing' implies protection of hardening concrete from excessive drying or freezing this term will not be used in this paper. Thermal treatment can be performed at different temperature and humidity under ambient pressure or water saturation pressure. The application of a specific temperature and corresponding water saturation pressure is referred to as 'hydrothermal treatment' or 'autoclaving'.

A thermal treatment of UHPC offers several advantages. As for ordinary concrete it accelerates the hardening process, but applying elevated temperatures is not connected with the risk of delayed ettringite formation known for ordinary concrete [14]. After the treatment, the hydraulic and pozzolanic reaction and the associated strength development is completed to a high degree [13–17]. After six years storage in water, however, Schachinger et al. measured a further increase in compressive strength of about 20% for heat treated UHPC samples compared to an increase of 58% for the specimens not subjected to heat treatment [18]. Thermal treatment leads to an enhanced hydration of the cement clinker and to an improved pozzolanic reaction of the siliceous additions, which consumes more calcium hydroxide at higher temperatures. Additionally, by the availability of water released with the decomposition of ettringite at temperatures above 70 °C [14, 19] the large amount of unhydrated cementitious components commonly remaining in hardened UHPC can be activated. In this way, the early strength is always considerably increased and in certain cases also the 28 days strength [13–15, 20–22]. The intensified pozzolanic and hydraulic reactions result in a denser and more homogeneous microstructure of the cement paste matrix corresponding to an improved durability [23]. Thermal treatment leads further to an improved dimensional stability because shrinkage is widely completed during treatment [24] and creep is significantly reduced [25].

The thermal treatment of UHPC is commonly performed as follows: right after demoulding at 12–48 h the components are steam-cured in a heating cabinet for 24–48 h at a temperature between 60 and 90 °C [12, 26–28]. These elevated temperatures and pressures offer the potential to improve strength development more efficiently [29–34]. Due to its very dense microstructure some authors attribute UHPC self-autoclaving properties when the temperatures of the thermal treatment exceed the boiling point [35]. Own research however showed substantial differences in flexural strength between UHPC treated at 250 °C and atmospheric pressure versus UHPC autoclaved at 200 °C. The strength loss is probably due to micro cracks resulting from high temperature and moisture gradients within the UHPC specimens in the initial heating and cooling phase [30].

Considering that higher temperatures and longer treatment times consume more energy and are less cost efficient, several authors suggest conditions for an optimal hydrothermal treatment regarding high (compressive) strength [13, 15, 29, 31, 33]. While Yungsheng et al. [34] suggest a dwell time of 8 h for a hydrothermal treatment at 200 °C and 1.7 MPa, Heinz et al. propose the same dwell time of 8 h at a temperature of 150 °C [33]. Yazıcı et al. analysed the

effect of a hydrothermal treatment on Reactive Powder Concrete (RPC) and recommend a slightly longer dwell time of 10 h at 180 °C / 1 MPa [29]. All authors agree that longer dwell times or higher pressure do not improve the strength significantly.

The above-mentioned studies, however, were not focused on thermal treatment but on mixture design or mechanical properties of UHPC, so that the findings are based only on a few parameter variations. Furthermore, the optimal conditions probably differ with different UHPC compositions [29, 33]. Aim of the study presented in this article was therefore to systematically analyse the impact of different thermal treatments on the phase composition of the hydrates and the resulting mechanical properties.

1.3 Phase development of UHPC

In principle, the general path of phase development in UHPC, i.e. the formation of hydration products, does not differ from normal concrete. The same phases occur in the same sequence, though the fractions of the individual phases and the kinetics are strongly different [27, 36]. Due to the low w/c ratio especially the amount of non-reacted clinker and supplementary cementitious materials is higher and conversely the degree of hydration is lower than for ordinary concrete.

The amorphous calcium silicate hydrates (C–S–H-phases) found in ordinary concrete as well as in UHPC depend on the chemical composition of the raw materials. Whereas hydration of pure Portland cement results in C–S–H-phases with a Ca/Si ratio of approx. 1.7 this ratio decreases for increasing replacement with SCMs [37]. The generic term C–S–H describes an indefinite range of semi-crystalline to nearly amorphous phases [38] which in concrete further vary depending on space (inner and outer C–S–H) and time of hydration.

It is generally recognized that thermal treatments at higher temperatures lead to an accelerated formation of C–S–H-phases, which is due to an accelerated reaction of cement clinker and SCMs, such as micro silica [13–15, 39]. The CaO/SiO_2 mole ratio of the mixture used amounts to 1.2 so that according to the phase diagram in Fig. 1 the crystalline phases tobermorite, xonotlite and afwillite are likely to be formed during heat treatment.

Knowledge regarding the impact of the treatment with temperatures above the boiling point of water, or with hydrothermal treatment on the phase composition of UHPC is however less consolidated. Yazıcı et al. attributed the high strength of autoclaved reactive powder concrete to the formation of tobermorite [29]. Glasser and Hong [41, 42] performed thermodynamic experiments in the C–S–H system, which also evidenced the occurrence of tobermorite at 200 °C under water vapour saturation. Luke [43] analysed oil-well cement blended with fly ash and microsilica and reported similar results. Research of Lehmann [31] indicated that in hydrothermally treated UHPC basically the same phases occur like in aerated autoclaved concrete (AAC) or calcium silicate bricks (CSB). Like Yazici [11] he further reported a decrease in strength after prolonged hydrothermal treatment. While Lehmann relates the strength loss to grain size growth, Yazici attributes it to the transformation of tobermorite and xonotlite to other crystalline C–S–H-phases.

In the presented study it was of special interest how far the phase composition of autoclaved UHPC shows analogies to the mineralogy of the traditionally autoclaved materials AAC and CSB.

1.4 Phase development of traditionally autoclaved building materials

AAC and CSB are based on calcium-silicate systems and are industrially produced by autoclaving process since 1894 (CSB) respectively since 1920 (AAC). The influence of the process parameters on the development of the hydration products and the composition of phases in these materials is well known. Besides quartz and calcite from the raw materials, portlandite, ettringite or monosulphate are present as well as crystalline C–S–H-phases, such as tobermorite ($Ca_5Si_6O_{16}(OH)_2{\cdot}4H_2O$), α-$C_2SH$ ($Ca_2O{\cdot}SiO_2$), xonotlite ($Ca_6Si_6O_{17}(OH)_2$), afwillite ($Ca_3Si_2O_4(OH)_6$) or gyrolite ($NaCa_{16}Si_{23}AlO_{60}(OH)_8{\cdot}64(H_2O)$) as characteristic products of the hydrothermal treatment. Typical and envisaged is the formation of 11 Å-tobermorite, which is associated with high strength [44, 45]. The formation of hydration products is depending on material composition (mainly Ca/Si ratio) and temperature (Fig. 1) as well as the duration of the hydrothermal treatment.

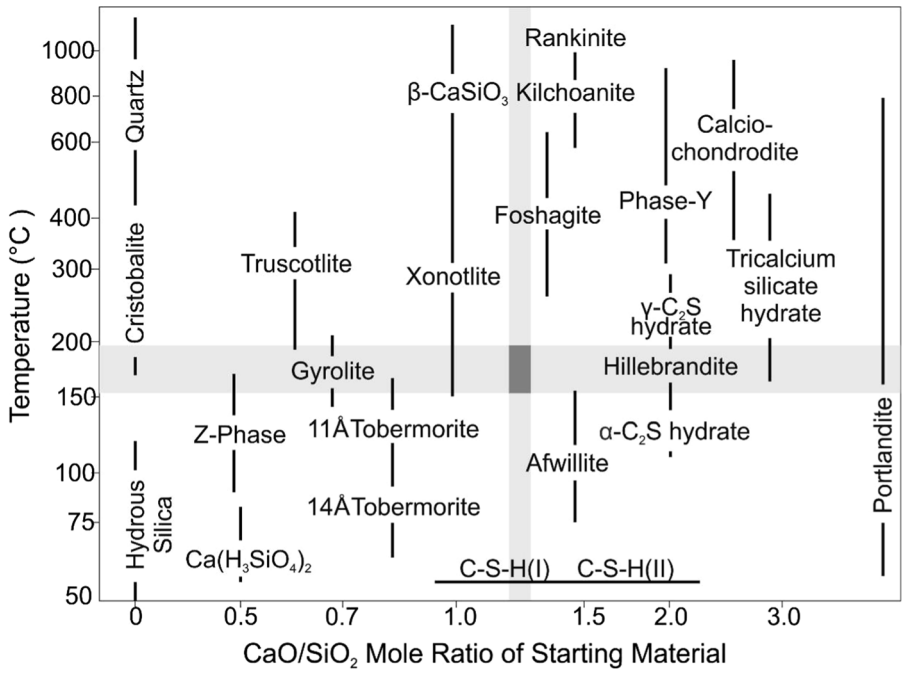

Fig. 1 CaO–SiO_2-phases subject to the CaO/SiO_2-ratio of the starting material after [40]. As emphasized by Meller the figure does not represent an equilibrium diagram but merely represents the condition under which each phase is most usually obtained. Marked in grey are the region of interest for hydrothermal treatment (*y*-axis) and the CaO/SiO_2-ratio of 1.2 correlating with the concrete mix (*x*-axis). For better readability the logarithmic axes labels are not to scale

Applying the hydrothermal conditions used in the production of AAC, metastable tobermorite is formed [46] by the reaction of ground quartz sand either with portlandite or with C–S–H-phase. Under equilibrium conditions tobermorite decomposes to xonotlite and quartz, which significantly decreases the compressive strength of the building material [47]. This undesired xonotlite formation during AAC production is attributed to unfavourable selection of the raw materials as well as to excessively high autoclaving temperatures or autoclaving times [47–50].

According to Sakiyama et al. [51] the addition of gypsum to the lime-quartz mixture for CSB promotes the formation of hydroxylellestadite, which later in the autoclaving process reacts with quartz and decomposes to tobermorite and anhydrite. Due to this phase transitions the strength development is initially delayed, and finally, because of a finer microstructure a higher strength is achieved [51].

2 Materials and methods

2.1 UHPC composition and sample preparation

The UHPC composition used in this study is given in Table 1. The formulation of the mixture is following the mixture "M2Q" developed by Bornemann et al. [52].

Due to its superior granulometry limestone powder is often included as filler into the mix design. Also, different SCMs like fly ash and ground granulated blast furnace slag are frequently used as constituents for UHPC. These additions, however, change the Ca/Si ratio and therefore the path of phase formation during autoclaving. To keep the system as simple as possible and to adjust the CaO–SiO_2 ratio in the range favourable for tobermorite formation (Fig. 1), only pure silicious additions resp. fillers were used in the following study.

After mixing in a 10 L volume high energy mixer the UHPC was cast in silicone moulds to produce small cylindrical specimens with a diameter and a height of 22.6 mm (Fig. 2). The choice of these—even

Table 1 Composition of UHPC, modified after [52]

Material	Content (kg/m^3)
CEM I 52.5 R	832
Microsilica (uncompacted)	135
Quartz powder (0–0.125 mm)	207
Quartz sand (0–0.5 mm)	975
PCE (superplasticizer solid content 35% by mass)	40 (14 + 26)
Water	209

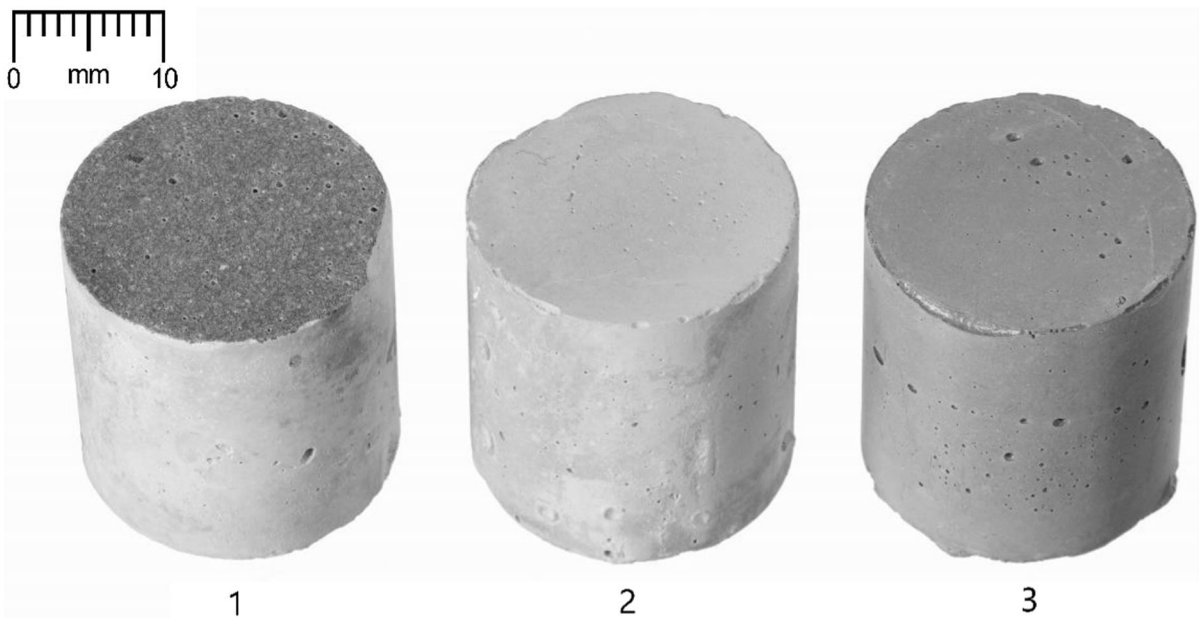

Fig. 2 Cylindrical samples used for strength tests and XRD: (1) after polishing the top surface, (2) after hydrothermal treatment, (3) before hydrothermal treatment

for fine grained concrete—very small dimensions has several reasons. Due to their small geometry, more specimens can be autoclaved at one time and the samples can be heated and cooled without inducing major temperature gradients inside the specimens. Furthermore, regular test equipment for concrete testing can be used for the mechanical testing of the high strength specimens. To compensate for the higher variation resulting from the use of small specimens eight samples were produced in each series for averaging.

In addition to the small cylindrical specimens, standard prismatic specimens (40 × 40 × 160 mm^3) were cast for investigating the effect of thermal treatment on compressive strength. For the bigger samples each series consisted of three samples. Results are presented in [15].

One day after preparation, the samples were demoulded and stored under water (23 °C) until thermal or hydrothermal treatment. After thermal treatment, the samples were stored in the water bath at 23 °C again until mechanical testing and phase analysis. For reference, UHPC samples were continuously stored under water at 23 °C after demoulding for 28 days. For better comparability the phase composition and the mechanical strength of all samples were analysed after 28 days, regardless of the pre-storage time before the hydrothermal treatment and the duration of the treatment.

2.2 Thermal treatment

In contrast to conventional concrete, UHPC is known to be not susceptible to the risk of monosulphate

formation and subsequent delayed ettringite formation when thermal treatment is carried out at temperatures up to 90 °C [14]. Thus, in this study thermal treatment was performed at a temperature of 90 °C, which is the upper limit used in practise according to [53].

To analyse the impact of the protection against drying, three series of specimens were analysed. The first series was stored unprotected in the heating cabinet and the second one vacuum-sealed with plastic foil. To obtain optimum curing conditions, i.e. optimum water availability, a third test series was stored in water during the treatment at 90 °C. For all sample series the pre-storage time before thermal treatment in the water bath at 23 °C was varied between 1 and 7 days and the dwell time of the heat treatment between 1 and 144 h.

2.3 Hydrothermal treatment

Hydrothermal treatment was performed in a laboratory autoclave (volume: 640 ml) at 185 °C with the corresponding water vapour pressure of 1.1 MPa. The heating rate was 1.5 K/min and the cooling rate was 0.3 K/min for all samples.

As in the test series for the thermal treatment, the pre-storage time before autoclaving (between 1 and 27 days) and the dwell time (up to 8 days) were varied. The shortest hydrothermal treatment comprised heating up the samples to the maximum temperature followed by immediate cooling without dwell time.

2.4 Phase analysis

Qualitative and quantitative phase analysis by solid sample XRD is based on two central assumptions [54]: First, the crystallites are ideally randomly oriented and second, there are enough crystallites to reach a representative intensity distribution, which is equivalent to a small crystallite size.

For ceramic or mineral samples these requirements are usually met by proper milling and sample preparation. In principle it is also possible to measure a solid sample directly if the above-mentioned preconditions can be ensured.

The crystallites in UHPC can be supposed as omnidirectional because the grains of the raw material are randomly arranged, and the hydration products grow without preferred directions into the voids. However, the grain size in the solid sample cannot be determined easily. Bigger crystallites could originate from the raw material or arise during hydration. In case the autoclaved samples contain unreacted quartz with the maximum grain size 0.5 mm, this will for sure cause irregular intensity ratios in the diffractograms. The even distribution of the other phases can be checked by two-dimensional X-ray Powder Diffraction (2D-XRD).

The phase analysis was carried out in Bragg–Brentano-Geometry with a DTex-detector and Cu-$K\alpha$ radiation. The samples were either milled to powder as a reference or measured as a solid sample (Fig. 3). Solid samples were polished with ethanol to obtain a smooth and homogeneous surface and fixed to a special sample holder. To enhance the statistics the solid samples were randomly twisted and measured for several times [55].

To analyse the effect of the crystallite size, a reference sample of the standard UHPC mixture (Table 1) was compared to a sample prepared without quartz sand (paste) using a General Area Detector Diffraction System (GADDS). The system combines a two-dimensional detector with a very small spot size. In case of an even distribution of crystallites the 2-D-recordings show concentric rings of homogeneous intensity. In contrast, big grains or texture are visualized by spottiness and inhomogeneous intensity along the rings as shown in the recording at the bottom of Fig. 4. For the two-dimensional analysis the same solid samples were used as for the standard XRD analysis. (Fig. 4).

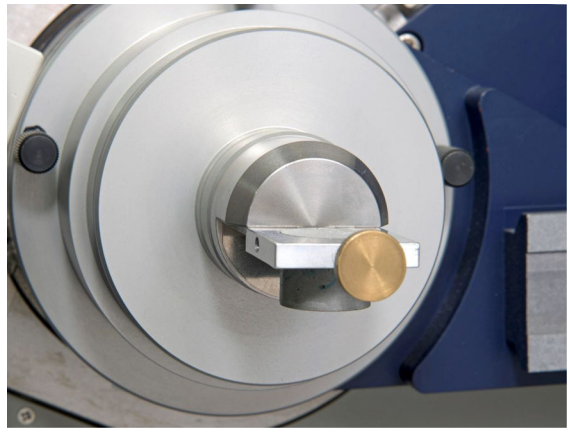

Fig. 3 Sample holder with UHPC cylinder for XRD phase analysis

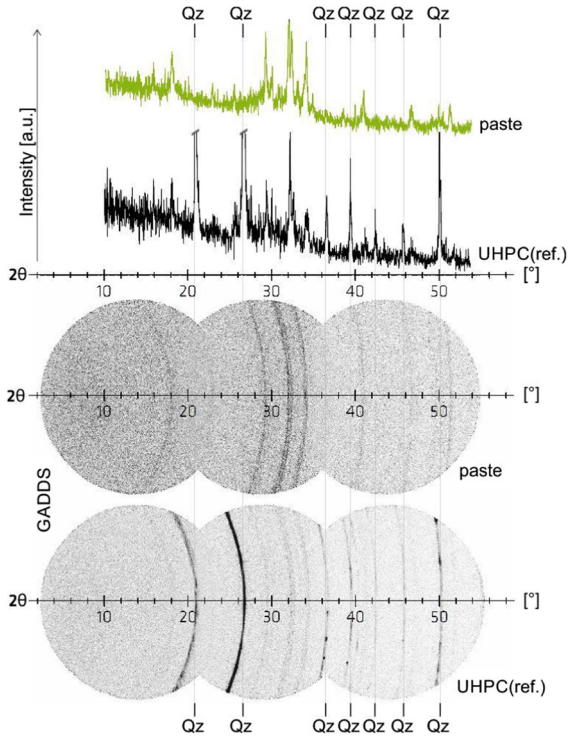

Fig. 4 Comparison of GADDS recordings of a solid sample of the UHPC reference mixture (bottom) and the identical paste mixture without quartz (middle) and X-ray-diffractograms determined by integration of the corresponding GADD recordings (top)

3 Results and discussion

3.1 XRD measurement conditions

The results from the powder diffraction and the measurement of the solid samples exhibit no significant differences regarding the presence and position of peaks. The feasibility of fast qualitative phase analysis using solid samples for the fine grained mixture used is described in detail in a separate publication [55].

The GADDS recording of the standard UHPC mixture is shown at the bottom of Fig. 4 and exhibits significant spots within the rings, e.g. at 21° 2θ, 36,2° 2θ, 39.8° 2θ and 50.1° 2θ, which are due to some oversized particles of quartz. The main peak of quartz around 27° 2θ (Fig. 4, top) appears as a continuous bold line (Fig. 4, bottom). Several further homogeneous rings, e.g. at 18° 2θ or around 32° 2θ, are only faintly visible and much more prominent in the paste sample. They can be attributed to cement phases or hydration products (Fig. 4, top and middle). Despite the dominant quartz peaks, all peaks relating to the crystalline hydrates visible in the paste sample can be clearly and unambiguously determined also in the UHPC sample (Fig. 4, top and bottom).

From the results, it can be concluded that the measurement of the UHPC cylinders in commonly used Bragg–Brentano-Geometry results in not representative intensities for the coarse quartz fraction but includes all reflexes and correct intensity ratios for the other phases. Therefore, a qualitative analysis is feasible also in samples containing quartz sand. The measurement of the solid specimens is more time efficient and preserves delicate minerals from changes due to harsh milling. Furthermore, it allows the depth-resolved measurement of thin layers or deposits on the surface as well as the reuse of the samples for further investigations. Due to these advantages solid samples were used in all further measurements.

3.2 Phase composition and compressive strength after thermal treatment

The XRD analysis of the reference sample, which was stored for 28 days in water at 23 °C, confirms the phase development described in literature [27, 36]: Corresponding to ordinary concrete, portlandite, ettringite and clinker phases can be identified in Fig. 5. Also, the amorphous hydrate phases and unconsumed microsilica are only visible as increased background in the area between 25° 2θ and 35° 2θ.

Due to the low *w/c* ratio and the high clinker content the proportion of not hydrated clinker phases is much higher than in conventional concrete.

The analysis of thermally treated samples shows that storage for 20 h in hot water of 90 °C leads to a significant decrease of ettringite and portlandite. The amount of not hydrated clinker phases in contrast does not change compared to the reference (Fig. 5). If the dwell time is increased to 144 h the amount of portlandite further decreases, whereas the clinker phases further remain at the same level. The fact that after this long dwell time there is still portlandite left implies potential for a further increase of the compressive strength with time due to pozzolanic reaction. For both heat-treated samples there are no peaks which can be assigned to crystalline C–S–H-phases like tobermorite (main peak at ~ 7.2° 2θ for 11 Å-tobermorite [56]), xonotlite (main peak at 28.9 [57])

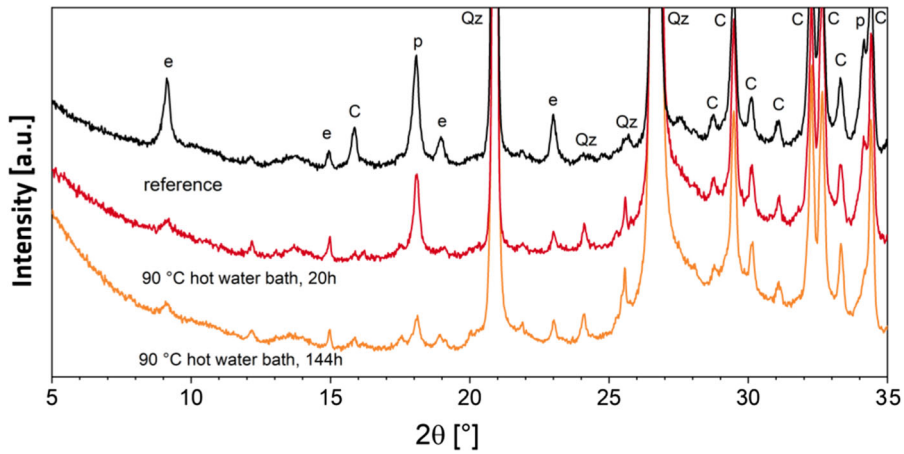

Fig. 5 Extracts from diffractograms (5°–35° 2θ) of a reference sample stored in water at 23 °C (black) and samples, which were treated in hot water at 90 °C for 20 h (red) and 144 h (orange). *E* ettringite, *p* portlandite, *Qz* quartz, *C* clinker phases. (Color figure online)

or afwillite (main peak at ~ 28.2° 2θ [58]) that could be expected in this temperature range and the CaO/SiO_2 mole ratio of the starting material of 1.2 according to Fig. 1. The XRD results indicate that the amount of water, which becomes available due to the decomposition of ettringite at temperatures above 70 °C, is used exclusively for an increased pozzolanic reaction of portlandite with microsilica, forming additional C–S–H-phases. The amount of water appears too low to promote a further hydraulic reaction of the cement clinker. The fact that Heinz and Ludwig did not observe portlandite already after a thermal treatment of 22 h at the same temperature, is probably due to the higher content of silica fume in the UHPC mixture used in their study [14].

Figure 5 further shows that ettringite is significantly reduced after a thermal treatment at 90 °C but not completely decomposed even after a duration of 144 h. The remaining amount of ettringite seems to be independent from the duration of the thermal treatment and is probably due to the specific characteristics of the material and experiment. The stability of ettringite depends in a complex manner on the specific boundary conditions like temperature, pressure and relative humidity as well as on its crystallite size and perfection [59]. In a dense matrix like UHPC decomposition is therefore in addition to temperature to a significant extent controlled by the very low rate of water migration. The importance of water for the pozzolanic reaction is further highlighted by the results of the mechanical testing after 28 days as shown in Fig. 6. While the compressive strength of the specimens, which were treated in the heating cabinet without any protection, is below the value of the reference samples of 175 MPa (represented by the dotted line indicating 100% in Fig. 6), the strength of the samples heat-treated in the water bath is up to 20% higher. The compressive strength of the sealed samples, which are protected from drying but cannot uptake additional water like the samples in the water bath, is still up to 10% higher than the reference value (Fig. 6). Contrary to earlier studies [17] the achievable

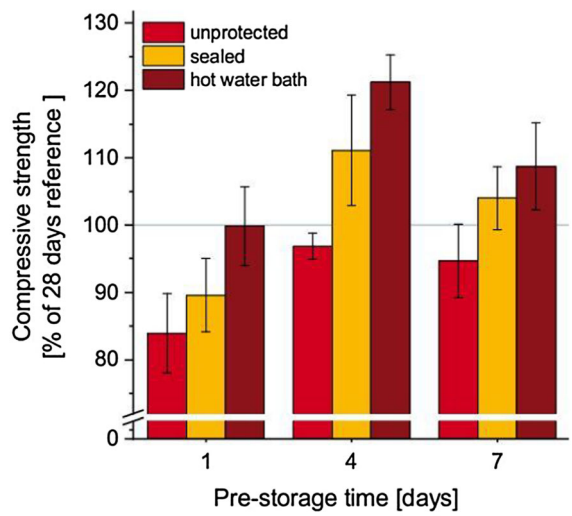

Fig. 6 Compressive strength of heat-treated cylindrical specimens (144 h at 90 °C) after 28 days depending on protection against drying and pre-storage times in percentage of the reference strength (175 MPa)

compressive strength also depends from the pre-storage time before the thermal treatment. It is assumed that a well-developed basic matrix favours strength development during heat treatment. Furthermore, additional water taken up during the pre-storage time can enhance the hydration process and mitigate autogenous shrinkage. Both factors increase strength development. The optimum pre-storage time, however, turned out not to be universal but to depend in a complex manner on the protection against drying as well as on the dwell time of the treatment. For the mixture analysed it ranges between 2 and 4 days. The measured differences in compressive strength related to the water availability are further only valid for the small sample geometry chosen. As described in detail in [15], the impact of the protection against evaporation on the achievable strength level is much smaller for prismatic samples with the dimension $40 \times 40 \times 160$ mm^3. Within a further study the prismatic specimens characterized by a visible zonation were analysed in detail with respect to chemistry, microstructure and mineral composition [60]. The results illustrate that for the specimens concerned which were treated without protection at 90 °C, there is an increase in compressive strength but a significant decrease in bending strength compared to the reference samples stored in water at 23 °C or in air with 50% relative humidity. Further investigations of the zone of visible zonation in comparison to the core of the specimens revealed changes in microstructure but no changes in crystallization products.The observation that the impact of the protection against evaporation on the mechanical strength is dependent from the geometry of the sample and even more important from the storage conditions after the thermal treatment has practical implications for the manufacturing process. While thermal treatment without protection may lead to a decrease in compressive strength only in case of structures with thin cross-sections, massive elements can suffer from an adverse effect in bending strength due to the formation of an outer layer with disturbed microstructure.

If there is protection against desiccation, the strength level increases with the duration of the thermal treatment (Fig. 7) [15]. It can be assumed that a continued treatment beyond the 144 h leads to a further improvement of strength as the hydration reactions of the clinker and the pozzolanic additions continue.

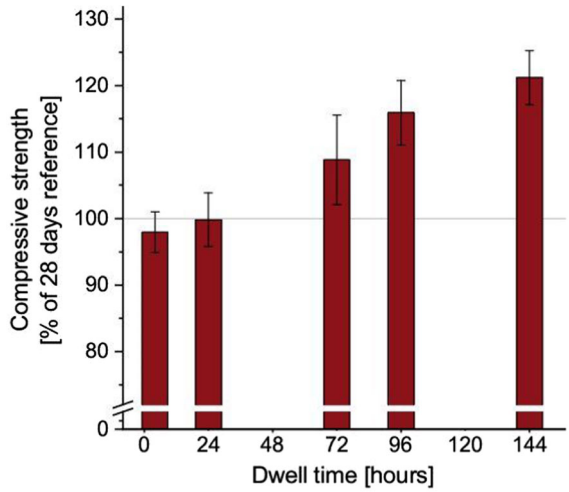

Fig. 7 Relative compressive strength of cylindrical specimens with a pre-storage time of 4 d depending on dwell time in hot water bath

3.3 Phase composition and compressive strength after hydrothermal treatment

During hydrothermal treatment at 185 °C and corresponding saturation vapour pressure the phase composition changes rapidly. Already after a dwell time of 4 h portlandite and ettringite have vanished and the amount of clinker phases is reduced. With increasing dwell time, the amount of clinker phases further decreases and the two new crystalline phases hydroxylellestadite and hydrogarnet appear. Even after an unrealistically long dwell time of 120 h a considerable amount of clinker phases is still left (Fig. 8). The sulphate and the aluminate stemming from the decomposition of ettringite are bound within the mineral phase hydroxylellestadite ($Ca_5(SiO_4)_{1,5}(SO_4)_{1.5}OH$) and the hydrogarnet ($Ca_3Al_2(SiO_4)(OH)_8$), respectively. Contrary to the findings of Sakiyama [61] the hydroxylellestadite is not decomposed into tobermorite and anhydrite as in CSB, but stable over the complete dwell time of 120 h. The permanent binding of the sulphate in the newly formed hydroxylellestadite could allow the use of sulphate bearing raw materials and is subject of further research.

Unexpectedly and contrary to the results of previous research [31, 32] and the literature reviews [14, 41, 42], no crystalline phases like foshagite, hillebrandite, tobermorite and afwillite were detected

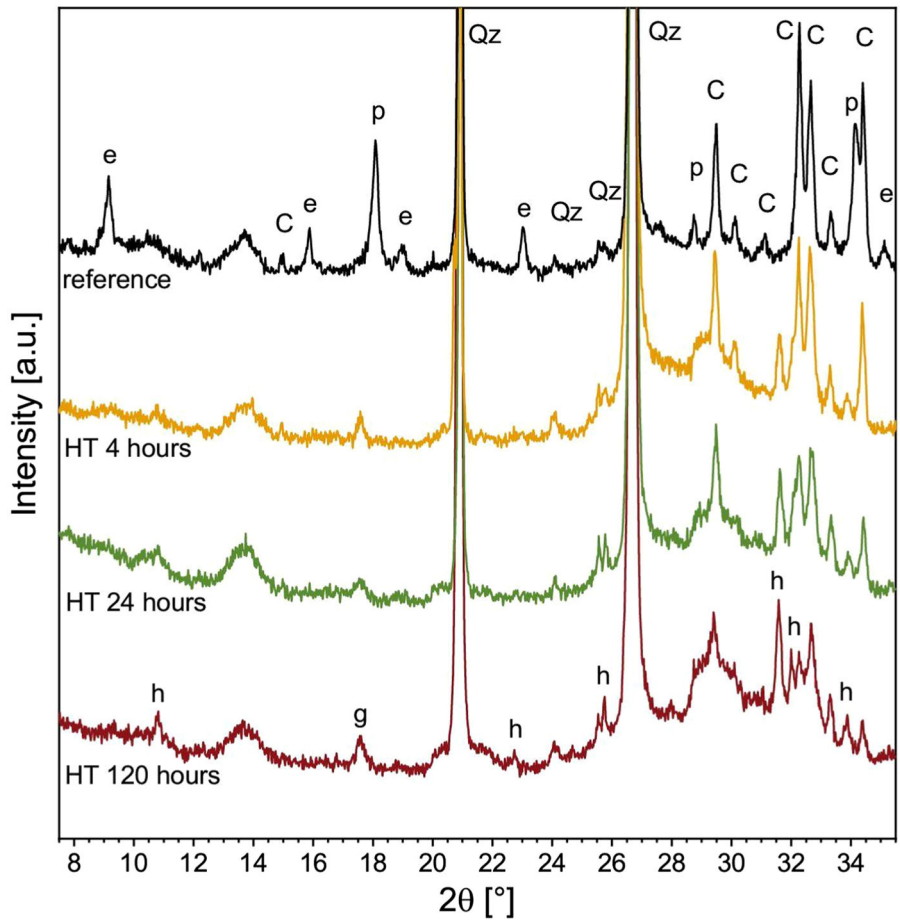

Fig. 8 X-ray diffractograms of small cylindrical UHPC samples hydrothermally treated for 4 h, 24 h and 120 h (dwell time) (185 °C/1.1 MPa) in comparison to the reference sample stored in water at 23 °C. *e* ettringite; *C* clinker, *p* portlandite, *h* hydroxylellestadite, *g* hydrogarnet, *Qz* quartz

in the bulk of the small cylindrical specimens. The absence of these phases could be due to the sample size. While Lehmann [31] was analysing the phase composition of prismatic specimens of $40 \times 40 \times 160\ mm^3$ hydrothermally treated in an industrial autoclave, in this study the XRD analysis was performed on small cylindrical samples treated as described in chapter 2.3 in a laboratory autoclave. The small sample size minimized the temperature and water vapour pressure gradients across the cross section and thereby changed the thermal and hygric boundary conditions, probably suppressing the formation of crystalline phases like reported by Feylessoufi et al. [39].

To identify the composition of the thin white layer (Fig. 2—sample 2) on the sample surface, which had formed during autoclaving, one solid sample was measured as it was taken out from the autoclave. The analysis (Fig. 9) showed calcite with a very prominent calcite peak at 29.4°2θ, which is formed quickly due to the reaction of portlandite with the airborne carbon dioxide. The second phase detected in the deposit of the surface was the 11 Å tobermorite with the main peak at 7.2° 2θ [62]. Due to the obvious Ca-saturation at the surface, it can be assumed, that the Ca-rich endmember of the tobermorite group with the chemical formula $Ca_5Si_6O_{17}{\cdot}5H_2O$ is formed. The difference between the phase composition at the surface and in the bulk material (Fig. 9) could only be detected with the new measuring strategy of solid samples which was introduced by Simon et al. [55]. When

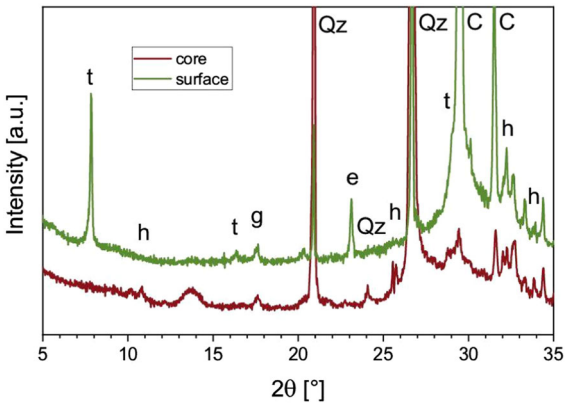

Fig. 9 X-ray diffractograms of hydrothermally treated UHPC samples (185 °C/1.1 MPa) with and without surface layer. *t* tobermorite, *e* ettringite, *C* clinker, *h* hydroxylellestadite, *g* hydrogarnet, *Qz* quartz

measured as a powder sample the phase is homogenized and a spatial localisation is impossible.

The occurrence of tobermorite at the surface confirms the temperature and pressure conditions for the genesis described in the phase diagram (Fig. 1). Its absence in the bulk of the sample must therefore be due to differences in chemistry, microstructure or thermal and hygric boundary conditions. The authors assume a combination of these three reasons as explained in the following.

(1) Different authors report that the formation of the strengthening 11 Å tobermorite is favoured by a reduced raw density [63–65]. The bigger pore space associated therewith allows a faster penetration of water vapour if there is a gradient across the sample cross section. Because tobermorite is built from the liquid phase its formation in the bulk material is most likely inhibited by water shortage and the high density of the samples used here. In contrast, enough water is available for crystallization at the surface.

(2) Due to the optimization of the packing density UHPC is characterized by a very dense microstructure. According to own investigations by mercury intrusion porosimetry [66] most pores have a radius smaller than 10 nm while the most frequent radius is 3 nm. C–S–H-phases crystallizing in these small pores cannot be measured with the X-ray diffractometer used. Using Cu-$K\alpha$ radiation the detection of tobermorite without significant peak broadening requires crystallite sizes bigger than 100 nm. Due to lack of space crystals of this size cannot be identified in the bulk material but only at the surface.

(3) As stated in the introduction the C–S–H phases developing during hydration depend on the chemistry of the raw materials but also vary depending on location and time. A further reason for the absence of tobermorite in the core could therefore be that the molar ratio of calcium to silicon is too high (Ca/Si $>$ 0.83), so that other (amorphous) C–S–H-phases are formed. At the surface however, the calcium content is slightly reduced by leaching so that the molar ratio is now in the right range for the formation of tobermorite. The detection of calcite at the surface of the specimen underscores the assumption that calcium was depleted by leaching and quickly reacted with the carbon dioxide of the surrounding air.

The strength development with increasing dwell time shown in Fig. 10 illustrates that already heating up the specimens to 185 °C in saturated steam atmosphere followed by an immediate cooling leads to an increase in compressive strength compared to the reference sample cured for 28 days in water. Strength improvement increases with dwell time up to 24 h. A

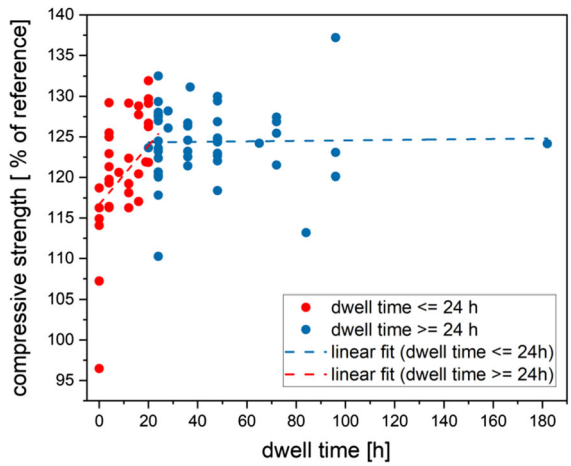

Fig. 10 Compressive strength of hydrothermally treated UHPC cylinders (185 °C/1.1 MPa) as function of dwell time (0–182 h) and pre-storage time (1–26 days) in percentage of the reference strength (175 MPa). The data is split in two sets: strength values resulting to dwell times from zero to 24 h (blue) and dwell time reaching from 24 h till 182 h (orange). (Color figure online)

very long dwell time of more than one week showed no further increase but the average compressive strength remains on the same level. The pre-storage time turned out to be insignificant when a minimum duration of several hours is met.

From the results, it can be concluded that the significant increase in compressive strength observed (Fig. 10) is due to an increased pozzolanic reaction of the portlandite with the siliceous fillers as well as an increased hydraulic reaction of the remnant clinker (Fig. 8).

The decisive prerequisite for both reactions is the availability of water, which after the consumption of the mixing water originates from the decomposition of ettringite. In contrast to the thermal treatment, the amount of water in a saturated steam atmosphere is enough to further increase the formation of C–S–H-phases also by hydraulic reaction. The newly formed C–S–H-phases are filling pores and cracks and thereby consolidate and homogenize the microstructure [32]. The finding that strength development is insensitive to long dwell times contrasts with the results of other researchers who observed a significant strength loss for specimen which were autoclaved over a longer time span [29, 31]. Complementary no new crystalline phases besides hydroxylellestadite and hydrogarnet were found in the small cylindrical samples treated for more than one week (Fig. 8). As hydroxylellestadite and hydrogarnet are already formed after a short autoclaving time a transition of crystalline phases as cause for the minor decrease in strength with time seems to be unlikely.

Tobermorite, which is known to be the main strength building phase in AAC and CSB was only found within the white deposit at the surface of samples, which had formed during the hydrothermal treatment. Within the bulk of the samples no tobermorite could be identified with XRD.

4 Conclusion

The research results show that strength development is strongly influenced by the level of protection against desiccation. In case of unlimited water availability during thermal treatment at 90 °C (hot water bath) compressive strength of the small cylindrical specimens can be increased by up to 20% compared to the reference samples stored in water at 23 °C. If the specimens are thermally treated in an oven and protected against drying sealed by a foil, the achievable increase reduces to 10%. If the protection against drying is omitted the compressive strength does not even reach the reference value.

For reaching an optimum strength gain, it seems to be advantageous that the specimens have developed a basic matrix during several days of pre-storage. The increase in strength can be attributed to an intensified pozzolanic reaction of the siliceous fillers, which is visualized by a decreasing portlandite peak with increasing dwell time. Thus, the hydration and pozzolanic reaction leading to a corresponding strength development can be promoted by an extended dwell time.

In case of hydrothermal treatment, already the short heating of the samples without dwell time increases compressive strength by about 15%. The maximum increase compared to the reference strength of about 30% is reached after autoclaving for 20 h. For the specimens treated hydrothermally, strength improvement can be ascribed to an increased pozzolanic reaction of the siliceous fillers as well as an increased hydraulic reaction of the clinker.

The water necessary for the formation of additional C–S–H-phases is mostly stemming from the decomposition of the ettringite. Whereas after treatment in hot water a 90 °C there is still portlandite and a small amount of ettringite left after 6 days, it takes only 4 h of autoclaving to consume both phases. The fact that after a dwell time of 120 h in saturated steam atmosphere there is still a considerable amount of clinker phases left, points to the availability of water as the limiting factor for the hydraulic reaction. The dense microstructure of the UHPC prevents that after the decomposition of the ettringite water is transported into the bulk of the sample.

Tobermorite as the main crystalline C–S–H-phase of AAC and CSB was not found in the bulk, but only in a thin layer at the surface of the hydrothermally treated samples. The cause for the spatial differentiation is probably a combination of the availability of water and pore space eventually supported by a different molar ratio of calcium to silicon caused by leaching of calcium.

Only in the hydrothermally treated samples hydroxylellestadite and hydrogarnet can be found as new formed phases. These new phases seem to permanently bind the sulphate and the aluminate stemming

from the decomposition of the ettringite. To support the hypothesis, that the use of sulphate bearing raw materials does not affect the durability of UHPC, further research is required.

Acknowledgements The study was financially supported by the Deutsche Forschungsgemeinschaft (DFG) (Grant ME 1461/11-1). The authors thank Christian Selleng and Katja Gröger for assisting and conducting part of the experiments.

Funding Open Access funding enabled and organized by Projekt DEAL.

References

1. SIA (2015) 2052: Ultra-Hochleistungs-Faserbeton (UHFB) – Baustoffe. Bemessung und Ausführung, Zürich
2. ASTM (2017) C1856/C1856M–17: standard practice for fabricating and testing specimens of ultra-high performance concrete. West Conshohocken, PA
3. Yanagida R, Nakamura T, Kono K, Niwa J (2017) Mechanical properties of fibre reinforced pore free concrete with high strength matrix above 400 MPa. Paper presented at the AFGC-ACI-fib-RILEM international symposium on ultra-high performance fibre-reinforced concrete UHPFRC 2017, Montpellier, France
4. Ricciotti R, Pastor F, Hajar Z, Bernardi S (2017) La Republique bridge in Monpellier. Paper presented at the AFGC-ACI-fib-RILEM international conference on ultra-high performance fibre-reinforced concrete UHPFRC 2017, Montpellier, France
5. Henry KA, Heany CW (2017) Industrialized production of thin rainscreen cladding in UHPC. Paper presented at the AFGC-ACI-fib-RILEM international symposium on ultra-high performance fibre-reinforced concrete UHPFRC 2017 Montpellier, France
6. Doiron G (2017) UHPC Pier repair/retrofit: examples of completed projects in North America. Paper presented at the AFGC-ACI-fib-RILEM international conference on ultra-high performance fibre-reinforced concrete UHPFCR 2017, Montpellier, France
7. Designing and Building with UHPFRC (2011). Wiley
8. Habert G, Arribe D, Dehove T, Espinasse L, Le Roy R (2012) Reducing environmental impact by increasing the strength of concrete: quantification of the improvement to concrete bridges. J Clean Prod 35:250–262. https://doi.org/10.1016/j.jclepro.2012.05.028
9. Sbia LA, Peyvandi A, Lu J, Abideen S, Weerasiri RR, Balachandra AM, Soroushian P (2016) Production methods for reliable construction of ultra-high-performance concrete (UHPC) structures. Mater Struct. https://doi.org/10.1617/s11527-016-0887-4
10. Camiletti J, Soliman AM, Nehdi ML (2012) Effects of nano- and micro-limestone addition on early-age properties of ultra-high-performance concrete. Mater Struct 46(6):881–898. https://doi.org/10.1617/s11527-012-9940-0
11. Yazıcı H (2007) The effect of curing conditions on compressive strength of ultra high strength concrete with high volume mineral admixtures. Build Environ 42(5):2083–2089. https://doi.org/10.1016/j.buildenv.2006.03.013
12. NPCA (2013) Ultra high performance concrete (UHPC): guide to manufacturing architectural precast UHPC elements. Carmel, IN, USA
13. Kang S, Lee J, Hong S, Moon J (2017) Microstructural investigation of heat-treated ultra-high performance concrete for optimum production. Materials 10(1106):13
14. Heinz D, Ludwig H-M (2004) Heat treatment and the risk of DEF delayed ettringite formation in UHPC. In: Schmidt M, Fehling E, Geisenhanslüke C (eds) Proceedings of the international symposium on ultra high performance concrete. Schriftenreihe Baustoffe und Massivbau, vol Heft 3. Kassel University Press, Kassel, pp 717–730
15. Selleng C, Meng B, Gröger K, Fontana P (2017) Influencing factors for the effectivity of heat treatment of ultra-high performance concrete (UHPC). Beton- und Stahlbetonbau 112(1):12–21. https://doi.org/10.1002/best.201600059
16. Yang SL, Millard SG, Soutsos MN, Barnett SJ, Le TT (2009) Influence of aggregate and curing regime on the mechanical properties of ultra-high performance fibre reinforced concrete (UHPFRC). Constr Build Mater 23:8
17. Ahlborn TM, Misson DL, Peuse EJ, Gilbertson CG (2008) Durability and strength characterization of ultra-high performance concrete under variable curing regimes. Paper presented at the 2nd international symposium on ultra high performance concrete, Kassel, Germany
18. Schachinger AI, Hilbig H, Stengel T (2008) Effect of curing temperature at an early age on the long-term strength development of UHPC. Paper presented at the 2nd international symposium on ultra high performance concrete, Kassel, Germany
19. Collepardi M (2003) A state-of-the-art review on delayed ettringite attack on concrete. Cem Concr Comp 25(4–5):401–407. https://doi.org/10.1016/S0958-9465(02)00080-X
20. Fehling E, Schmidt M, Walraven J, Leutbecher T, Fröhlich S (2014) Ultra-high performance concrete UHPC: fundamentals, design, examples. Beton-Kalender Series. Ernst & Sohn, Berlin
21. Kono K, Nakayama R, Tada K (2015) Development of the world's highest strength cementitious material. J Res Taiheiyo Cem Corp 169:20–29

22. Esmaeili J, Kasaei J (2016) Effect of different curing regimes on strength and transport properties of UHPC containing recycled steel tire wires as micro steel fibers. First international symposium on UHPC. Des Moines, Iowa, USA
23. Ahlborn TM, Harris DK, Misson DL, Peuse EJ (2011) Characterization of strength and durability of ultra-high-performance concrete under variable curing conditions. Transp Res Rec 2251:68–75. https://doi.org/10.3141/2251-07
24. Li W, Huang Z, Hu G, Hui Duan W, Shah SP (2017) Early-age shrinkage development of ultra-high-performance concrete under heat curing treatment. Constr Build Mater 131:767–774. https://doi.org/10.1016/j.conbuildmat.2016.11.024
25. Garas VY, Kurtis KE, Kahn LF (2011) Creep of UHPC in tension and compression: effect of thermal treatment. Cem Concr Comp 34:10
26. Association Francaise de Génie Civil (2013) Ultra High Perfomance Fibre-Reinforced concretes: Recommendations (Bétons fibrés à ultra-hautes perfomances: Recommandations). Documents scientifiques et techniques, Association Francaise de Génie Civil (AFGC), Paris
27. DAfStb (2008) Sachstandsbericht Ultrahochfester Beton, vol 561. DAfStb-Heft. Beuth Verlag GmbH, Berlin. http://d-nb.info/988918501
28. Soliman AM, Nehdi ML (2010) Effect of drying conditions on autogenous shrinkage in ultra-high performance concrete at early-age. Mater Struct 44(5):879–899. https://doi.org/10.1617/s11527-010-9670-0
29. Yazıcı H, Deniz E, Baradan B (2013) The effect of autoclave pressure, temperature and duration time on mechanical properties of reactive powder concrete. Constr Build Mater 42:53–63. https://doi.org/10.1016/j.conbuildmat.2013.01.003
30. Müller U, Kühne H-C, Meng B, Nemecek J, Fontana P (2008) Micro texture and mechanical properties of heat treated and autoclaved Ultra High Performance Concrete (UHPC). Paper presented at the 2nd international symposium on ultra high performance concrete, Kassel, Germany
31. Lehmann C (2013) Neue Perspektiven für Ultra-Hochleistungsbeton durch gezielte Beeinflussung des Nanogefüges. Dissertation, Technische Universität Berlin/BAM Bundesanstalt für Materialforschung und -prüfung, Berlin
32. Fontana P, Lehmann C, Müller U (2009) Influence of hydrothermal curing on micro structure and mechanical properties of ultra-high performance concrete. Paper presented at the 9th international symposium on brittle matrix composites, Warsaw, Poland
33. Heinz D, Urbonas L, Gerlicher T (2012) Effect of heat treatment method on the properties of UHPC. Paper presented at the 3rd international symposium on UHPC and nanotechnology for high perfomance construction materials, Kassel, Germany, 7–9. March 2012
34. Yunsheng Z, Wei S, Sifeng L, Chujie J, Jianzhong L (2008) Preparation of C200 green reactive powder concrete and its static-dynamic behaviors. Cem Concr Comp 30:8
35. Dehn F (2004) Temperature behaviour of ultra high-performance concrete (UHPC)—a micro analytical reflect. Paper presented at the proceedings of the international symposium on ultra high performance Concrete, Kassel
36. Korpa A, Kowald T, Trettin R (2009) Phase development in normal and ultra high performance cementitious systems by quantitative X-ray analysis and thermoanalytical methods. Cem Concr Res 39(2):69–76. https://doi.org/10.1016/j.cemconres.2008.11.003
37. Richardson IG (1999) The nature of C-S-H in hardened cements. Cem Concr Res 29(8):1131–1147. https://doi.org/10.1016/S0008-8846(99)00168-4
38. Chen JJ, Thomas JJ, Taylor HFW, Jennings HM (2004) Solubility and structure of calcium silicate hydrate. Cem Concr Res 34(9):1499–1519. https://doi.org/10.1016/j.cemconres.2004.04.034
39. Feylessoufi A, Crespin M, Dion P, Bergaya F, Van Damme H, Richard P (1997) Controlled rate thermal treatment of reactive powder concretes. Adv Cem Mater 6(1):21–27. https://doi.org/10.1016/s1065-7355(97)00006-0
40. Meller N, Kyritsis K, Hall C (2009) The mineralogy of the $CaO–Al_2O_3–SiO_2–H_2O$ (CASH) hydroceramic system from 200 to 350 °C. Cem Concr Res 39(1):45–53. https://doi.org/10.1016/j.cemconres.2008.10.002
41. Glasser FP, Hong SY (2003) Thermal treatment of C-S–H gel at 1 bar H_2O pressure up to 200 °C. Cem Concr Res 33(2):271–279. https://doi.org/10.1016/S0008-8846(02)00959-6
42. Hong SY, Glasser FP (2004) Phase relations in the $CaO–SiO_2–H_2O$ system to 200 °C at saturated steam pressure. Cem Concr Res 34(9):1529–1534. https://doi.org/10.1016/j.cemconres.2003.08.009
43. Luke K (2004) Phase studies of pozzolanic stabilized calcium silicate hydrates at 180 °C. Cem Concr Res 34(9):1725–1732. https://doi.org/10.1016/j.cemconres.2004.05.021
44. Matsui K, Kikuma J, Tsunashima M, Ishikawa T, Matsuno S-y, Ogawa A, Sato M (2011) In situ time-resolved X-ray diffraction of tobermorite formation in autoclaved aerated concrete: Influence of silica source reactivity and Al addition. Cem Concr Res 41:510–519
45. Arabi N, Jauberthie R, Chelghoum N, Molez L (2015) Formation of C-S-H in calcium hydroxide-blast furnace slag-quartz-water system in autoclaving conditions. Adv Cem Res 27(3):153–162. https://doi.org/10.1680/adcr.13.00069
46. Gabrovsek R, Kurbus B, D. M, Wieker W (1993) Tobermorite formation in the system CaO, C3S-SiO2-Al2O3-NaOH-H2O under hydrothermal conditions. Cem Concr Res 23. https://doi.org/10.1016/0008-8846(93)90097-S
47. Bernstein S (2011) Determination of reaction kinetics and mechanisms of 1.13 nm tobermorite by in-situ neutron diffraction. Ludwig-Maximilians-Universität, München
48. Fan J, Cao D, Jing Z, Zhang Y, Pu L, Jing Y (2014) Synthesis and microstructure analysis of autoclaved aerated concrete with carbide slag addition. J Wuhan Univ Technol Mater Sci Ed. https://doi.org/10.1007/s11595-014-1034-0
49. Smalakys G, Siauciunas R (2018) The synthesis of 1.13 nm tobermorite from carbonated opoka. J Therm Anal Calorim 134(1):493–502. https://doi.org/10.1007/s10973-018-7418-1
50. Galvankova L, Masilko J, Solny T, Stephankova E (2016) Tobermorite synthesis under hydrothermal conditions. Proc Eng 151:100–107

51. Sakiyama M, Oshio Y, Mitsuda T (2000) Influence of gypsum on the hydrothermal reaction of lime-quartz system and on the strength of autoclaved calcium silicate product. J Soc Inorg Mater Jpn 7(289):685–691. https://doi.org/10.11451/mukimate2000.7.685
52. Bornemann R, Schmidt M, Fehling E, Middendorf B (2001) Ultra high performance concrete UHPC—composition, properties and applications. Beton- und Stahlbetonbau 96(7):458–467. https://doi.org/10.1002/best.200100550
53. DAfStb (2012) Wärmebehandlung von Beton. DAfStb-Richtlinie, Ausgabe November 2012 edn. Deutscher Ausschuss für Stahlbeton e.V. - DAfStb, Berlin
54. Buhrke VE, Jenkins R, Smith DK (eds) (1998) A practical guide for the preparation of specimens for x-ray fluorescence and x-ray diffraction analysis. Wiley-VCH, New York
55. Simon S, Selleng C, Meng B (2018) Prompt phase analyses of ultrahigh-performance concrete. J Mater Civ Eng. https://doi.org/10.1061/%28ASCE%29MT.1943-5533.0002163
56. Houston JR, Maxwell RS, Carroll SA (2009) Transformation of meta-stable calcium silicate hydrates to tobermorite: reaction kinetics and molecular structure from XRD and NMR spectroscopy. Geochem Trans 10:1. https://doi.org/10.1186/1467-4866-10-1
57. Ge Z, Yao X, Wang X, Zhang W, Yang T (2018) Thermal performance and microstructure of oil well cement paste containing subsphaeroidal konilite flour in HTHP conditions. Constr Build Mater 172:787–794. https://doi.org/10.1016/j.conbuildmat.2018.03.268
58. Zhang TT, Zhao YL, Wang W, Yi H, Li HQ, Zhang QW, Song SX (2017) A novel model of aggregate gradation for autoclaved bricks from tailings. Minerals. https://doi.org/10.3390/min7070112
59. Zhou Q, Glasser FP (2001) Thermal stability and decomposition mechanisms of ettringite at < 120°C. Cem Concr Res 31:1333–1339
60. Voigt M, von Werder J, Meng B (2020) Investigation of the zonation of thermally treated ultra high performance concrete. Constr Build Mater 254. https://doi.org/10.1016/j.conbuildmat.2020.119187
61. Sakiyama M, Oshio Y, Mitsuda T (2000) Influence of quartz particle size and lime/quartz ratios on the strength of autoclaved calcium silicate board. Applied Mineralogy, Vols 1 and 2: Research, Economy, Technology, Ecology and Culture. A a Balkema Publishers, Leiden
62. Biagioni C, Merlino S, Bonaccorsi E (2015) The tobermorite supergroup: a new nomenclature. Mineral Mag 79(2):485–495. https://doi.org/10.1180/minmag.2015.079.2.22
63. Gundlach H, Hörster E, Radermacher G (1969) Der Einfluss der Reaktionsraumgröße bei der Hydrothermalsynthese der Caliumsilikathydrate. Tonindustrie-Zeitung und Keramische Rundschau 93(3):107–114
64. Eden W (2011) Einfluss der Verdichtung von Kalk-Sand-Rohmassen auf die Scherbenrohdichte von Kalksandsteinen (Influence of the compaction of calcium silicate raw materials on the structural density of calcium silicate masonry units), vol Heft 15. Schriftenreihe Baustoffe und Massivbau, vol Heft 15. Kassel University Press, Kassel
65. Hartmann A, Buhl JC, van Breugel K (2007) Structure and phase investigations on crystallization of 11 Å tobermorite in lime sand pellets. Cem Concr Res 37(1):21–31. https://doi.org/10.1016/j.cemconres.2006.09.007
66. Rübner K, Klobes P, Prinz C, Hempel S (2006) Charakterisierung der Porenstruktur von ultrahochfestem Beton. Paper presented at the XIII. Workshop über die Charakterisierung von feinteiligen und porösen Festkörpern, Bad Soden, 14.-15.11.2006